Indian J. Phys. **75A** (4), 379-383 (2001)

IJP A
an international journal

Magnetism in a new series of high-energy-density magnetic materials of amorphous alloys

S Ram
Materials Science Centre, Indian Institute of Technology, Kharagpur, Kharagpur-721302, West Bengal, India

E-mail : sram@matsc.iitkgp.ernet.in

Abstract : Unusually, a high-energy-density $(JH)_{max}$ as 10 to 20 kJ/m^3 appears in amorphous R-Fe-Al alloys at room temperature. This is a new series of ferromagnets that presents a considerably high value of $(JH)_{max}$ in an amorphous state. The present $(JH)_{max}$ value is comparable to that in well-known high-energy-density rare-earth (R) magnets of $R_2Fe_{14}B$ and similar intermetallics. In principle, a high value of $(JH)_{max}$ occurs on a high value of coercivity H_c and/or remanence J_r. A primary source of H_c is the magnetocrystalline anisotropy H_a which appears in a crystalline ferromagnetic (or ferrimagnetic) material. It results in an optimal value of H_c in an assembly of single domain particles of size $D \sim D_c$, with D_c the critical value of D. As an amorphous material does not have H_a it is not expected to have a large value of H_c observed in this example. This is demonstrated with representative R-Fe-Al (R = Nd, Pr, or Er) amorphous alloys. The values of H_c, J_r, Curie temperature, T_C, as well as $(JH)_{max}$ are found to be optimal at an optimal Fe ~ 30 at % content over the series.

Keywords : Magnetism, amorphous alloys, high energy density

PACS No. : 75.50.Kz, 75.50.Ww, 75.50.Vu

1. Introduction

A tremendously high value of energy-density, $(JH)_{max}$, of 200 to 500 kJ/m^3 often appears in $R_2Fe_{14}B$, RM_5, or R_2M_{17} intermetallics [1-8], where R is a rare-earth and M is transition metal element. In principle, an optimal value of $(JH)_{max}$ or coercivity H_c occurs in an assembly of single domain particles of size $D \sim D_c$, with D_c the critical value of D. The value of H_c decreases regularly on smaller as well as on bigger D values. A value of $D_c = 20$ nm has been reported in a pure ferromagnetic Fe, Co, or Ni metal [9]. A more or less similar value of D_c also appears in the present intermetallics [5-8]. In principle, a high value of H_c, *i.e.*, as large as 50 kA/cm, in this series occurs due to a high value of magnetocrystalline anisotropy H_a. In general, H_a is as large as an order of larger magnitude of H_c [4,8].

Very recently, Inoue *et al* [10-12] introduced an amorphous series of R-Fe-Al alloys that presents unexpectedly a large 10 to 20 kJ/m^3 value of $(JH)_{max}$. The amorphous phase forms in a wide composition range of 0 to 90 at % Fe and 0 to 93 at % Al by melt spinning [10]. A high H_c or $(JH)_{max}$ is reported in the $R_{90-x}Fe_xAl_{10}$, with R = Nd or Pr, compositions obtained by a copper mold casting method [10, 11]. Being isotropic in nature, they have an especial advantage over the above series of the intermetallics that they can be used also as isotropic magnets. This is presented in this article with synthesis and magnetic properties of R-Fe-Al bulk amorphous alloys, with R = Nd, Pr or Er. These alloys were prepared by two independent methods of arc melting [13] and mechanical attrition process [14] under high purity conditions. Both of them are the established methods for preparation of a bulk alloy [13-16].

2. Experimental details

As mentioned above, we prepared the amorphous bulk alloys by two independent methods of (i) arc melting and (ii) mechanical attrition process as follows. In method (i), the pure R, Fe and Al metals were mixed together in requisite amounts and then melted by an arc melting in an argon atmosphere. It yielded ingots of the R-Fe-Al alloy. The ingots were cut and crushed in small pieces of 1 to 3 mm diameter and then were remelted in a similar manner to ensure its chemical homogeneity. As described earlier [16], milling of a requisite mixture of the three metals (powders) in method (ii) gives a similar bulk amorphous bulk alloy.

The formation of the amorphous R-Fe-B bulk alloy phase in the two methods is analyzed by various metallographic techniques. The thermal stability of the amorphous structure is determined by the analysis of the structural parameters of $\Delta T = T_m - T_x$, which is desirably found to be as small as 90 K,

and T_m / T_x ratio, which is desirably extremely high as 0.9. Here, T_m and T_x are the onset of the melting and recrystallization temperatures of the alloy. Its chemical composition, amorphous structure, and microstructure are studied with electron microscopy (having the provision for electron microprobe analysis) and X-ray diffractometry. The magnetic properties, *ie.*, saturation magnetization J_S, H_c, J_r and Curie temperature T_C are studied with the help of a vibrating sample magnetometer. Other experimental details are the same as reported earlier [5-8].

3. Results and discussion

A. X-ray diffractogram and microstructure :

Unusually, the R-Fe-Al alloy easily forms in an amorphous structure if cooling from the melt in an inert atmosphere even at a slow 10 to 0.1 K/s rate. It is therefore easily achieved by using various kinds of solidification techniques, *e.g.*, water quenching, mold casting, high pressure die casting, arc melting, unidirectional arc melting, and suction casting [8-12]. The mechanical attrition of an elemental mixture in a controlled atmosphere, used in the present study, gives an altogether a different of away of vitrifying it in a bulk amorphous alloy without involving a melting of it. A small addition of a volatile additive of a hydrocarbon liquid during the attrition of significantly helps its vitrification in a refined amorphous structure. It facilitates the reaction between the refined metal particles with nascent surfaces and results in a finely divided loose powder in the vitrified alloy.

Figure 1 shows x-ray diffractograms of $Nd_{100-x}Fe_xAl_{10}$, $x \sim 30$, alloy obtained by the two different methods of (a) the arc melting and (b) the mechanical attrition process. A single broad diffraction halo, characteristic of an amorphous phase [12-14], appears in either case. The halo lies at diffraction angle 2θ = 32.3° or scattering vector k = 22.7 nm^{-1} (which is defined by $k = 4\pi \sin\theta / \lambda$, with $\lambda = 0.1505$ nm the wavelength of the radiation used to measure the diffractogram) with a bandwidth $\Delta 2\theta_{1/2} \sim 3.3^0$ in sample (a). That is very little shifted at lower $2\theta = 31.5^0$, or a lower k = 22.1 nm^{-1}, with $\Delta 2\theta_{1/2} \sim 4.3^0$ in sample (b). A similar diffraction halo occurs at a more or less

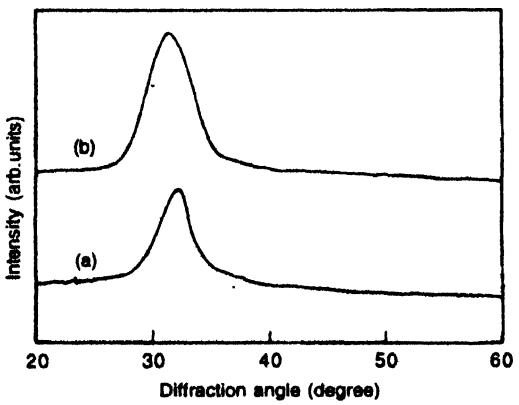

Figure 1. X-ray diffractograms of a hard ferromagnetic $Nd_{60}Fe_{30}Al_{10}$ amorphous alloy obtained by two different process of (a) arc melting and (b) mechanical attrition for 25 h in a pure argon atmosphere.

similar k-value in the alloy prepared by the suction casting method [10]. Also a melt spun ribbon in $Nd_{90-x}Fe_xAl_{10}$ ($x \sim 30$), or in a more general $R_{90-x}Fe_xAl_{10}$ alloy, which is believed to have a perfect amorphous phase, has a similar diffractogram of a broad halo at $k \sim 22$ nm^{-1} (cf. ref. 10 to 12). Average position of the diffraction halo does not change much on a change of R over a wide range of x.

The single broad halo of the diffractogram indicates a single prominent pair distribution function of the atoms in the $R_{90-x}Fe_xAl_{10}$ alloys. A marginal variation in its average position occurs in the specimens deduced with different methods owing to a marginal variation in their average interatomic distance d. The sample obtained through the mechanical attrition process therefore presents a smaller value of k = 22.1 nm^{-1} (a larger $d = \lambda / 2\sin\theta \equiv 2\pi\kappa^{-1}$ value) if compared with k = 22.7 nm^{-1} in that obtained by the arc melting process as it stores a large amount of excess energy $\Delta\varepsilon$ (or enthalpy ΔH) over the equilibrium value ε_0 in the forms of structural imperfections and defects during the attrition process. The excess $\Delta\varepsilon$ or ΔH results in an excess volume ΔV of the sample as per the first law of thermodynamics. This excess volume releases in a board exothermic structural relaxation signal if heating the sample in a thermal analyser as will be discussed later in section B.

In the attrition process of a mixture of R, Fe and Al metals (powder) in a predetermined composition, ball-powder-ball and ball-powder-container collisions repeatedly occur and plastically deform, cold-weld, and fracture the powder particles. Strain hardening and fracture of particles during the collisions create new surfaces by a decrease of their one or more dimensions according to the experimental conditions. When two or more refined surfaces in case come in contact react together instantly by dissolution of one component into other(s), and result in a vitrified alloy. The process is called mechanical alloying. Its scanning electron micrograph indicates a layered structure of it formed by a peculiar reaction within the components and a cold welding of latter in layer by layer [16].

The monolayer of the alloy gets as thinned as possible in the continuous collisions during the attrition process. As per usual microstructure in attrition of pure metals [16], it assumes a definite thickness (t), which appears to be smaller if compared with the critical diameter (D) in a stable crystallite of it, *i.e.*, $t < D$. In instantaneous cold-welding of a freshly created nascent layer structure over a stable layer supports its originally thin layered structure. As a result, the material in the thin layer does not recrystallize in the course of an extended milling process and the final sample ultimately succeeds to attain an amorphous structure in individual layers, which are arranged one over others. We analyzed transmission electron micrographs of selected samples with *in-situ* studies of their compositional maps and the corresponding electron diffraction patterns. A single amorphous structure, in composition of the alloy, appears throughout the specimen with a characteristic broad diffraction ring at k = 22.1 nm^{-1}, as observed in the x-ray diffractogram

(Figure 1). No impurities of a crystalline phase were observed in a significant 1% or larger trace.

A similar structureless feature of microstructure appears in the alloy obtained by the arc melting. It does not have distinct particle structures with defined boundaries expected in crystalline particles. No significant liquid-liquid phase separation or a precipitation is visible at a measurable scale. It appears that the alloy components are peculiarly highly soluble one into other and easily form a single stable homogeneous melt. The melt, therefore, easily retains its liquid structure even if cooling it slowly at ~ 1 K/s (which is easily obtained in this method) in small ingots of diameter as big as 4 to 5 mm diameter.

B. Phase diagram and strong glass formability :

As mentioned above, the $Nd_{90-x}Fe_xAl_{10}$ easily forms in an amorphous phase in ether method over the x series. For example, Figure 2 shows a DSC thermogram obtained for a typical $x = 30$ alloy obtained in small ingots of 4 to 5 mm diameter by the arc melting. It exhibits a broad exothermic peak over 500 to 750 K (with a change of enthalpy $\Delta H_1 = 12\,J/g$) followed by a strong exothermic peak at $T_p = 795$ K (with enthalpy $\Delta H_2 = 35\,J/g$) with $T_x = 763$ K and $T_m = 910$ K. The present T_x and T_m values are in a fairly good agreement with the values reported by other methods. The first signal is a characteristic structural relaxation signal with a large $\Delta H_1 = 12\,J/g$ excess energy retained in the alloy above its equilibrium energy state ε_0. The mechanical attrition process results in a presumably further larger value of $\Delta H_1 = 15\,J/g$ (with $T_p = 800$ K, $T_x = 760$ K and $T_m = 915$ K) stored in the alloy in the form of an excess energy in structural imperfection and defects with an enhanced volume in its deformed structure in thin layers.

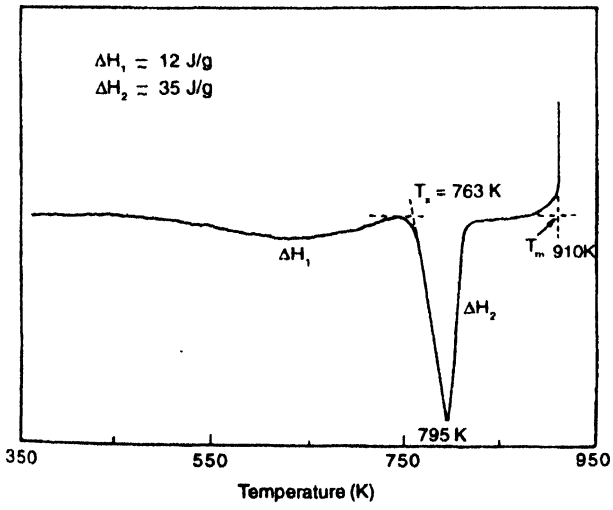

Figure 2. DSC thermogram of a hard ferromagnetic $Nd_{60}Fe_{30}Al_{10}$ amorphous alloys obtained by the arc melting process. The thermogram is recorded during heating the specimen at 0.33 K/s.

The values for T_x and T_m for the selected R-Fe-Al alloys are summarized in Table 1. The temperature interval, $\Delta T_m = T_m - T_x$, of the supercooled liquid defined by the difference between T_m and T_x is as small as 90 K and the reduced crystallization temperature $\Phi = T_x / T_m$ is as high as 0.9. The small ΔT_m and large Φ values seem to be responsible for the large glass forming ability in these alloys.

Table 1. Thermal stability data for the hard ferromagnetic R-Fe-Al amorphous bulk alloys

Composition	Thermal stability*			
	T_x(K)	T_m(K)	$\Delta T_m = T_m - T_x$	$\Phi = T_x / T_m$
$Nd_{70}Fe_{20}Al_{10}$	750	866	116	0.87
$Nd_{60}Fe_{30}Al_{10}$	763	910	147	0.84
$Pr_{60}Fe_{30}Al_{10}$	765	855	90	0.90
$Er_{60}Fe_{30}Al_{10}$	820	950	130	0.86

* The data are deduced from DSC thermograms measured at 0.33 K/s heating.

A large glass-forming ability in this system, leading to the formation of bulk amorphous alloy, originates from the high thermal stability of the liquid (or solid solution) against crystallization at T_x and above. It can be described by the temperature interval, $\Delta T_x = T_x - T_g$, of the supercooled liquid region before crystallization, where T_g is its glass transition temperature. Inoue *et al*[12] studied the compositional dependence of ΔT_x for a series of R-Fe-Al amorphous alloys. As proposed by these authors, the large glass forming ability in this series satisfies three empirical rules, (i) alloy systems consisting of multicomponents, (ii) significantly different atomic size ratios above 12% among the main constituent elements, and (iii) a large negative heat of mixing among the constituent elements. For example, a typical phase diagram for a multicomponent alloy series of soft magnetic materials, after Inoue *et al* [12], is reproduced in Figure 3. According to it, the largest value of ΔT_x = 49 K is obtained at the $Fe_{74}Al_4Ga_2P_{12}B_4Si_4$ composition. A Fe-rich $Fe_{80}P_{12}B_4Si_4$ composition has a smaller $\Delta T_x = 36$ K. Simultaneous dissolution of Ga and Al with larger atomic sizes and large negative heat of

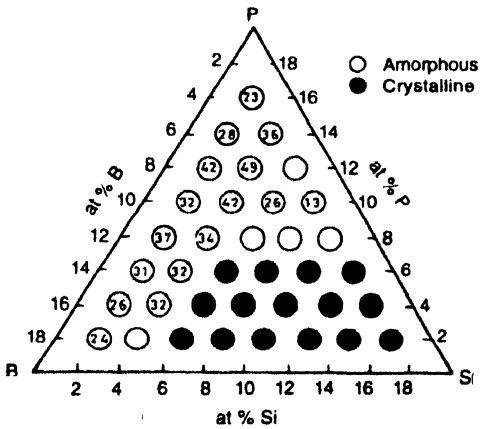

Figure 3. Phase diagram of an amorphous phase formation (soft ferromagnetic) in rapidly solidified $Fe_{74}Al_4Ga_2$ (P, B, Si)$_{20}$ alloys. The numbers represent the temperature interval, $\Delta T = T_x - T_g$, of the supercooled region.

mixing against the other constitutent elements is, therefore, very effective for extension of the ΔT_x region before the crystallization at T_x.

The alloy achieved with the extended ΔT_x = 49 K is truly amorphous in nature and it involves a large value of enthalpy of relaxation ΔH_{rel} in the T_g region in accord with the present results. The large value of ΔH_{rel} (*e.g.*, 15 J/g observed in the alloy in Figure 2) masks the relatively weak endothermic step of the T_g. It is, therefore, not visible in these examples. As shown in Figure 2, the excess ΔH_{rel} releases with a prominent exothermic structural relaxation signal on heating the sample through it. In general, the ΔH_{rel} signal is more prominent in shear vitrified alloys. All these alloys exist in nonequilibrium metastable states far above their equilibrium energy states ε_0. The excess ΔH_{rel} energy therefore releases in an exothermic relaxation signal on heating the sample through it. In an isothermal heating $T \leq T_g$, at , it results in a monotonically decreasing exothermic signal as a function of time. This has been studied and discussed with thermodynamic modeling in other reports in the series [14, 15].

The R-Fe-Al series presents an exceptionally extended phase diagram (Figure 4) of formation of an amorphous alloy over a wide compositional range. A thin amorphous ribbon easily forms at 0 to 90 at % Fe and 0 to 93 at % Al by rapid quenching [10]. Also a bulk amorphous alloy forms over a pretty wide range of 20 to 40 at % Fe and 10 to 30 at % Al by copper mold casting and other methods [10, 11]. The as cast ingots of the R-Fe-Al alloys, 4 to 5 mm diameter, by the arc melting in this work, therefore, have a smooth surface and a metallic luster at 20 to 40 at % Fe in formation of the amorphous phase. A systematic change in the atomic size of Nd>Fe>Al and large negative heats of mixing for Nd-Al, Al-Fe, and Nd-Fe atomic pairs support a large glass forming ability of it as per the above three empirical rules.

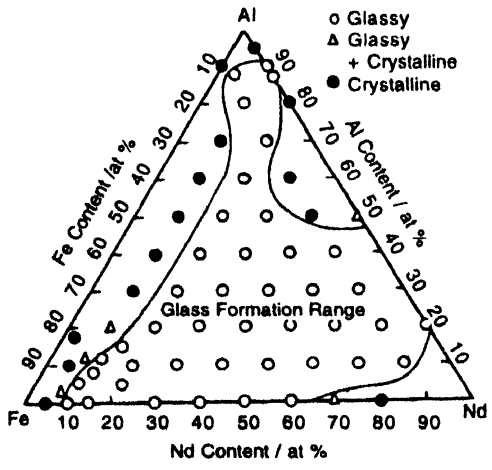

Figure 4. Phase diagram of an amorphous phase formation (hard ferromagnetic) in rapidly solidified Nd-Fe-Al alloys.

C. Magnetic properties :

The $R_{90-x}Fe_xAl_{10}$ alloy series irrespective of R exhibits optimal values of remanence J_r, saturation magnetization J_s, energy-product $(JH)_{max}$, and Curie temperature T_C at x ~ 30. As given in Table 2, the alloy with R = Nd has the highest value of $(JH)_{max}$ = 19 kJ/m^3 with the highest value of T_C = 610 K. T_C is a strong function of Fe-Fe, R-Fe and R-R exchange interactions of the

Table 2. Magnetic properties for the hard ferromagnetic R-Fe Al amorphous bulk alloys.

Composition	Magnetic properties			
	J_i(T)	H_c(kA/m)	$(JH)_{max}$ (kJ/m^3)	T_c (K)
$Nd_{70}Fe_{20}Al_{10}$	0.08	239	13.0	550
$Nd_{60}Fe_{30}Al_{10}$	0 12	277	19 0	610
$Pr_{60}Fe_{30}Al_{10}$	0.09	300	13.0	515
$Er_{60}Fe_{30}Al_{10}$	0.10	280	12.0	590

a) The optimal values appear in the amorphous bulk alloy at 30 at % Fe content.

magnetic R and Fe atoms in the system. As a result, it sensitively varies with a function of R as well as with a function of x in a given R-series. Pr($4f^2$), which has a smaller magnetic moment than Nd ($4f^3$), accounts for the smaller value of T_C (515 K against 610 K at x ~ 30) in the $Pr_{90-x}Fe_xAl_{10}$ alloy with respect to that in the $Nd_{90-x}Fe_xAl_{10}$ alloy (Table 2). Moreover, in thermomagnetograms in Figure 5, an increase in the value of x from (a) x = 20 to at (b) x = 30 in the $Nd_{90-x}Fe_xAl_{10}$ series leads to an increase in the T_C-value by 60 K with the final value of 610 K. According to it, the Fe-Fe exchange interactions have a more pronounced effect on T_C than the R-Fe or R-R exchange interactions.

The Pr-based alloy is characteristically more oxidation corrosion resistant than the Nd-based alloy in ambient atmosphere [8]. It therefore presents its stable magnetic properties. This is highly necessary for practical applications of these alloys in magnet technology and related devices and components. In this case, a partial substitution of Nd by Pr in the $(Nd_{1-y}Pr_y)_{90-x}Fe_xAl_{10}$ series thus could be a better alternative to have a practically useful alloy with its stable magnetic properties.

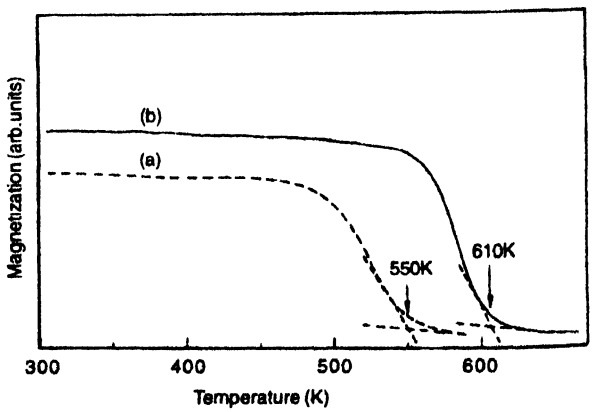

Figure 5. The thermomagnetograms showing a significant increase in the T_C value by 60 K with a mall 10 at % increase in Fe-content in ($Nd_{70}Fe_{20}Al_{10}$ and (b) $Nd_{60}Fe_{30}Al_{10}$ alloys.

4. Conclusions

Amorphous bulk R-Fe-Al alloys form a new class of high-energy-density (HED) magnetic materials. As compared to well-known $R_2Fe_{14}B$ intermetallics and other HED magnetic materials, the amorphous bulk alloys exhibit a relatively large electrical resistivity, which make them particularly suitable for applications in high frequency devices at a low power loss. The as-received amorphous bulk R-Fe-Al alloys present an energy-density as large as $(JM)_{max} \sim 19$ kJ/m^3, *i.e.* comparable to that for the conventional high frequency ceramic magnets. Unusually, the R-Fe-Al alloys if recrystallised behave to be extremely soft magnetic in nature and extremely hard in mechanical strength. Several unusual magnetic transitions appear at low temperatures in the virgin as well as in the recrystallised alloys with small crystallites at a nanometer scale. This is a subject of eminence academic interest nowadays in modeling of the dynamics of magnetic spins in correlated systems of small particles of a quantum confined size.

Acknowledgments

This work has been financially supported by a research grant from the Council of Scientific & Industrial Research (CSIR), Government of India.

References

[1] K Strnat, G Hoffer, J Olson, W Ostertag and J J Becker *J Appl Phys* **38** 1001 (1967)

[2] M Sagawa, S Fujimura, M Togawa and Y Matsuura *J Appl Phys* **55** 2083 (1984)

[3] J J Croat, J F Herbst, R W Lee and F E Pinkerton *J Appl Phys* **55** 2078 (1984)

[4] K Schnitzke, L Schultz, J Wecker and M Katter *Appl. Phys. Lett.* **56** 587 (1990)

[5] S Ram and J C Joubert *J Appl Phys* **72** 1164 (1992)

[6] S Ram *Phys Rev* **B 49** 9632 (1994)

[7] S Ram, E Claude and J C Joubert *IEEE Trans Magn* **31** 2200 (1995)

[8] S Ram *J Mater Sci* **32** 4133 (1997)

[9] W Gong, H Li, Z Zhao and J Chen, *J Appl Phys* **69** 5119 (1991)

[10] A Inoue, T Zhang, A Takeuchi and W Zhang *Mater Trans JIM* **37** 636 (1996)

[11] A Inoue, T Zhang and A Takeuchi *Mater Trans, JIM* **37** 1731 (1997)

[12] A Inoue, A Takeuchi and T Zhang *Metall Mater. Trans* **29A** 177 (1998)

[13] P S Frankwicz, S Ram and H J Fecht *Appl. Phys Lett* **68** 2825 (1996)

[14] S Ram and G P Johari *Phil Mag* **B61** 299 (1990)

[15] S Ram *Phys Rev* **B 42** 9582 (1990)

[16] S Ram and H J Fecht *Mater Trans JIM* **41** 754 (2000)